UNIVERSITY OF VAASA

FACULTY OF TECHNOLOGY

COMMUNICATIONS AND SYSTEMS ENGINEERING

Mariam Shukuru Kawambwa

PILOT CONTAMINATION MITIGATION TECHNIQUES IN MASSIVE MIMO SYSTEMS: A PRECODING APPROACH

Master's thesis for the degree of Master of Science in Technology submitted for inspection, Vaasa, 27 October, 2016.

Supervisor Professor Mohammed Elmusrati

ACKNOWLEDGMENT

First and foremost, I express my heartfelt gratitude to God Almighty. It is by His will that I have managed to produce this work.

Secondly, I would like to convey my sincere gratitude to my supervisor, Professor Mohammed Elmusrati, for his guidance throughout the development of this work and also throughout my Master's program. He has believed in me more than I have believed in myself and that gave me the courage to persevere whenever I hit roadblocks.

In addition, my sincere gratitude goes to the University of Vaasa and the Finnish government for offering me the opportunity to pursue my Master's degree in Finland.

I would also like to thank my lovely young brothers, Karim and Malik, and my friends for their continuous words of encouragement and motivation. They really brought some light to the dull days where I could not see the finish line.

Last but not least, my deepest appreciation goes to my beloved parents, Dr. Shukuru Kawambwa and Mrs. Saum Kawambwa, for their unconditional love and support and for providing me the opportunity to further my education in a country thousands of miles away from home. They are and have always been my greatest support system and there is nothing in this world that can fully express my appreciation other than my ever-lasting love and respect for them.

TABLE OF CONTENTS **page**

SYMBOLS

α_k	Complex magnitude of the channel fading coefficient between the BS and user *k*
θ_k	Azimuth angle of the plane wave from the k^{th} user
σ_n^2	Noise power at the receiver
ϕ_k	Azimuth angle of the plane wave from the k^{th} user
β	Phase propagation factor
$\Delta\Psi_M$	Phase difference between the signal received at base station antenna element *M* and the reference antenna element
λ	Wavelength of a signal
$\mathbf{a}_k$	Steering of the k^{th} user
C_k	Capacity achieved by the k^{th} user
d_k	Distance between the base station and user *k*
g_{ij}	Average channel gain between the i^{th} receiver and j^{th} transmitter
h_{ij}	Channel impulse response between the i^{th} receiver and j^{th} transmitter
$\mathbf{h}_k$	Channel impulse response vector between the base station antenna array and the k^{th} user
$\mathbf{n}_k$	Additive white Gaussian noise at the k^{th} user
P_r	Power received
$\mathbf{s}_k$	Payload for the k^{th} user
$\mathbf{w}_k$	Zero-forcing beamforming weight of the k^{th} user
$\mathbf{Y}_k$	Received signal at the base station antenna array, from the k^{th} user
D	Reuse distance
$\mathbf{H}$	Channel matrix
$\widehat{\mathbf{H}}$	Channel estimate
K	Number of simultaneously served users
M	Number of antennas at the base station
N	Cluster size
$\mathbf{N}$	Additive white Gaussian noise at the base station
P	Base station transmit power

R	Cell radius
u	Transmit vector from the base station

ABBREVIATIONS

16-QAM	16-ary Quadrature Amplitude Modulation
3D	three-dimensional
4G	4th generation
5G	5th generation
AWGN	Additive White Gaussian Noise
BER	Bit Error Rate
BS	Base station
BT-PCP	Beamforming Training and Pilot Contamination Precoding
CAGR	compound annual growth rate
CDI	Channel Distribution Information
CE	Channel Estimation
CSI	Channel state information
CSIT	Channel State Information at the Transmitter
dB	Decibels
DPC	Dirty Paper Coding
FDD	Frequency–Division Duplex
FSPL	Free Space Path Loss
H-inf	H-infinity
ISI	Intersymbol Interference
LS	Least Squares
LSFP	Large-Scale Fading Precoding
LTE	Long Term Evolution
MATLAB	Matrix Laboratory
MIMO	Multiple input multiple output
MISO	Multiple Input Single Output
MMSE	Minimum Mean Squared Error
mmWave	Millimeter wave
MRC	Maximum Ratio Combining
MU-MIMO	Multi-User Multiple Input Multiple Output

NMSE	Normalized Mean Square Error
OFDM	Orthogonal Frequency Division Multiplexing
PCEP	Pilot Contamination Elimination Precoding
PCP	Pilot Contamination Precoding
PiC	Pilot contamination
RAT	radio access technology
SDMA	Space-Division Multiple Access
SIMO	Single Input Multiple Output
SINR	Signal-to-Interference-plus-Noise Ratio
SISO	Single Input Single Output
SNR	Signal-to-Noise Ratio
TDD	Time–Division Duplex
UE	User equipment
UHD	Ultra-High Definition
ZF	Zero-Forcing

LIST OF FIGURES

LIST OF TABLES

UNIVERSITY OF VAASA
Faculty of Technology
Author: Mariam Shukuru Kawambwa
Topic of the Thesis: Pilot Contamination Mitigation Techniques in Massive MIMO Systems: A Precoding Approach
Supervisor: Professor Mohammed Elmusrati
Degree: Master of Science in Technology
Degree Program: Degree Programme in Communications and Systems Engineering
Major of Subject: Communications and Systems Engineering
Year of Entering the University: 2014
Year of Completing the Thesis: 2016 **Pages:** 54

ABSTRACT:

A massive MIMO system comprises of base stations with a very large number of antennas serving a considerably smaller number of users and providing substantial gains in spectral and energy efficiency in comparison to conventional MIMO systems. However, these benefits are limited by pilot contamination which is caused by the use of training sequences for channel estimation. This negative effect has given rise to various research works on schemes to mitigate pilot contamination and among them are precoding techniques.

This thesis reviews some of the precoding techniques that mitigate pilot contamination and studies the effect of pilot contamination on the performance of massive MIMO systems through simulations. It was found that pilot contamination leads to a severe degradation of the network performance. Furthermore, as the number of antennas at the base station increases, the effect of pilot contamination is more prominent on the probability of outage and the bit error rate but this is not the case for the average sum capacity. With the average sum capacity, the effect diminishes very gradually as the antenna array at the base station grows. However, overall, the presence of pilot contamination further lowers the network performance as the number of antennas at the base station increases.

KEYWORDS: Pilot contamination, precoding, massive MIMO

1. INTRODUCTION

As stated by Marzetta (2015), “two timeless truths are evident: first, demand for wireless throughput will always grow; second, the quantity of available electromagnetic spectrum will never increase.”

In recent years, the amount of traffic carried through mobile networks has been growing exponentially. The Cisco visual networking index (2016) indicates an estimated growth of 74 percent in global mobile data traffic in the year 2015. Based on a compound annual growth rate (CAGR) of 53 percent, the overall mobile data traffic is expected to grow to 30.6 Exabyte per month by 2020. This figure is a staggering eightfold increase over 2015.

One of the primary contributors to the global mobile traffic growth is an increase in the number of mobile devices connected to the wireless communication networks. In the year 2014, the number of mobile devices connected was estimated to be 7.3 billion. This figure grew to 7.9 billion in the year 2015. That is an increase of 600 million mobile devices in just one year. This figure is expected to reach 11.6 billion by the year 2020 at a CAGR of 8 percent. (Cisco visual networking index 2016.)

Another primary contributor, as stated by Rodriguez (2015), is the growing demand for advanced multimedia applications such as Ultra-High Definition (UHD) and three-dimensional (3D) video as well as augmented reality and immersive experience. In comparison to other content types, video content has relatively higher bit rates. Due to this, they are anticipated to generate the largest portion of the mobile traffic growth through 2020 (Cisco visual networking index 2016).

Such exponential growth in global mobile traffic has led to the advancement from the 4^{th} generation (4G) of mobile communications to the 5^{th} generation (5G). 5G mobile communications is expected to meet the ever-increasing high data rate and connectivity demands. It is expected to pave the way towards the 4^{th} stage of industrial revolution where the currently human-dominated wireless communications is extended to an all-

connected world of humans and objects (Monserrat, Dohler & Osseiran 2016). According to Rodriguez (2015), the first wave of 5G networks is expected to be operational around 2021 with expected peak data rate of 10Gbps. The high data rates will provide extensive connectivity with 'fiber-like' experience for the users.

With 5G, there are currently numerous research works on various feasible techniques to reliably and uniformly provide the ever-increasing total wireless throughput to all designated areas. Marzetta (2015) reports that the proposed solutions seem to fall into one of three categories:

- The exploitation of the high frequency bands (>6GHz) that are currently unused or underutilized.
- The deployment of more access points, each covering a relatively smaller cell.
- The use of access points and/or terminals with multiple antennas. This is termed Multiple Input Multiple Output (MIMO).

The first two solutions will not be discussed due to the fact that massive MIMO is the main area of focus in this thesis. Massive MIMO is the latter form of MIMO that is emerging as its ultimate and most useful form.

One of the major challenges that arise with the deployment of massive MIMO is pilot contamination (PiC). Massive MIMO systems operate in time-division duplex mode and use training sequences (also referred to as pilot signals) to estimate the channel. Consequently, pilot contamination occurs due to pilot reuse that significantly corrupts the channel state information (CSI) and in turn degrades the performance of the network. This challenge gives rise to extensive research on techniques to mitigate pilot contamination.

There are numerous PiC mitigation schemes that have been evaluated in literature due to the importance of accurate CSI and the strong negative impact of PiC on the quality of the acquired CSI. These schemes differ in various aspects such as complexity and modes of operation i.e. time, frequency or power domain. (Monserrat et al. 2016.)

The focus of this thesis is on the precoding schemes proposed with the objective of theoretically analyzing them and finally studying the effect PiC has on the performance of massive MIMO systems, through MATLAB simulations. A multi-cellular network, consisting of multiple users is simulated and analyzed by comparing its performance in the presence of PiC with its performance in the absence of PiC. The performance metrics used are probability of outage, average achievable sum capacity and bit error rate (BER). It should be pointed out that in this work, the terms *users* and *user equipment* (UE) are used interchangeably.

This work is sectioned into four main chapters.

- Chapter one highlights the motivation behind the research topic and its importance as well as the objective of the thesis. Additionally, a brief description of the analysis process is provided.
- Chapter two explains the major aspects of MIMO systems such as precoding, the channel and pilot contamination in order to create an understanding on the topic and the research works that are reviewed in the final section of the chapter.
- Chapter three describes the developed system model and the simulation process.
- Finally, in chapter four the simulation results are discussed and conclusions drawn. Furthermore, recommendations are made for future work.

2. LITERATURE REVIEW

2.1. Massive MIMO (Multiple Input Multiple Output)

According to Santos, Edwards-Block & Licea (2013) any wireless communication system can be categorized into four groups based on antenna configuration:

1. Single Input Single Output (SISO): single transmit and single receive antenna.
2. Single Input Multiple Output (SIMO): single transmit antenna and multiple receive antennas.
3. Multiple Input Single Output (MISO): multiple transmit antennas and a single receive antenna.
4. Multiple Input Multiple Output (MIMO): multiple transmit and multiple receive antennas.

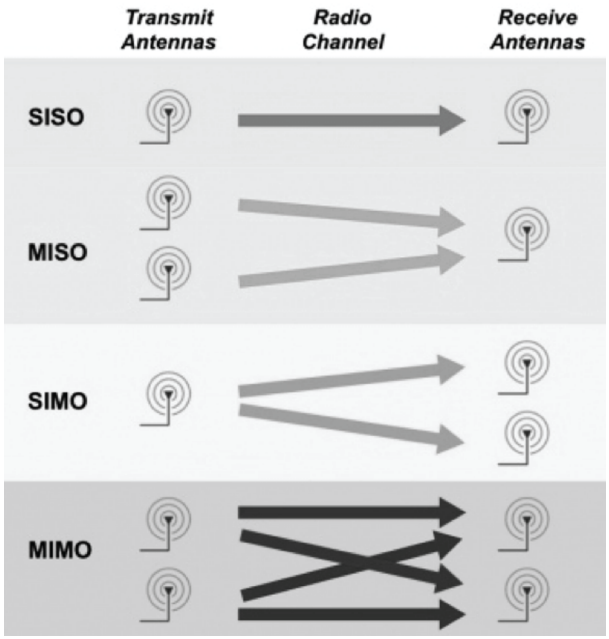

Figure 1. Antenna configurations (Santos et al. 2013).

Santos et al. (2013) continue to indicate that multiple antenna systems are implemented in order to attain the following:

- Diversity gain: This is the increase in the reliability of the wireless communication systems through the transmission or reception of signals via independently fading multiple paths. The system becomes more reliable due to the fact that the probability of deep fading is reduced with the increasing number of independent links.
- Array/beamforming gain: This is the average increase in the receiver signal-to-noise ratio (SNR) through coherently combining the signals from multiple antennas at the receiver and/or the transmitter.
- Spatial multiplexing gain: This is the increase in data rate without the need of higher transmission power. This can be achieved through, for instance, the transmission of multiple data streams that are spatially multiplexed into the same frequency-time resource.

The diversity, beamforming, and multiplexing gains achieved by the use of multiple antenna systems have been revolutionary to the wireless communications industry. The current emerging multiple antenna technology is massive MIMO. It is a scaled up version of MIMO by orders of magnitudes hence achieving even higher gains.

Massive MIMO is a form of Multi-User MIMO (MU-MIMO). The term multi-user arises from the fact that instead of employing a single transmitter and receiver each with multiple antennas, as is with traditional (point-to-point) MIMO, the single receiver with multiple antennas is split into multiple receivers each with typically a single antenna as shown in Figure 2. Consequently, during the uplink, the system is seen as multiple SIMO networks and in the downlink, the system is seen as multiple MISO networks.

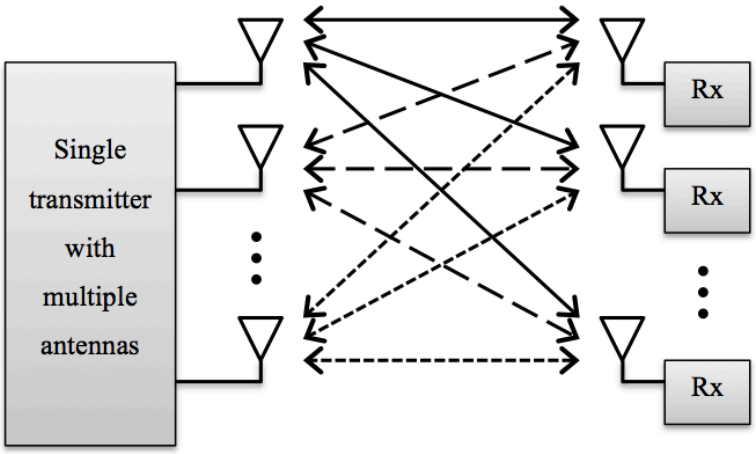

Figure 2. Multi-User MIMO.

Massive MIMO has been defined in a couple of ways. Some groups define it as any MIMO configuration that exceeds those implemented in current long term evolution (LTE) systems; at present 8x8. On the other hand, other groups simply refer massive MIMO to the implementation of a large array of antennas at the base stations. However, the best way to define massive MIMO is by relating it to the ratio of serviced users to the number of antennas that are serving those users. In order to achieve the benefits of multi-antenna systems, the number antennas at the base station should be more than or equal to the number of users being simultaneously served by the base station. (Panzner, Zirwas, Dierks, Lauridsen, Mogensen, Pajukoski & Miao 2014.)

Larsson, Edfors, Tufvesson & Marzetta (2014) explain that massive MIMO systems rely on spatial multiplexing, which in turn rely on the base station acquiring information on the channel state in both the uplink and downlink. This information is known as channel state information (CSI). CSI at the base station is used to perform precoding on the downlink data streams before transmission as shown in figure 3.

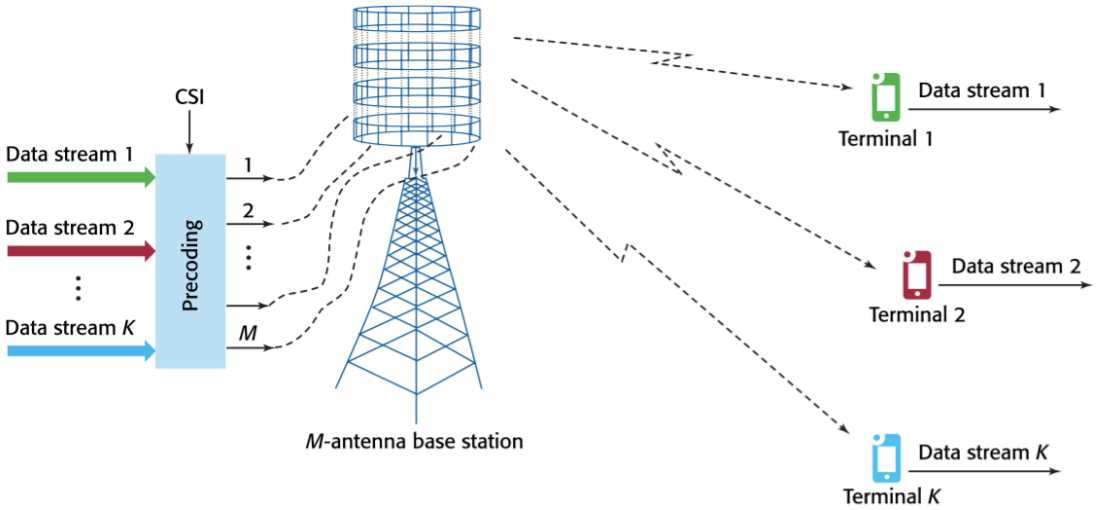

Figure 3. Downlink operation of a massive MIMO link (Marzetta 2015).

Marzetta et al. (2014) continue to explain that on the uplink, the acquisition of the CSI can easily be accomplished by having the terminals transmit their assigned pilots to the base station where they are used to estimate the channel responses to each of the terminals. However, the downlink is more challenging due to the magnitude of antennas at the base station. In conventional MIMO systems, pilot sequences are transmitted from the base station to the terminals where they are used to estimate the channel responses and the results are fed back to the base station. Unfortunately, this is not practical in massive MIMO systems for the following reasons:

- The amount of time-frequency resources required for downlink pilots is directly proportional to the number of antennas at the base station due to the fact that optimal downlink pilots ought to be mutually orthogonal between the antennas. Therefore, in comparison with a conventional MIMO system, a massive MIMO system would require much more such resources.
- The number of channel responses to be estimated by each terminal scales with the number of base station antennas. In turn, the uplink resources needed to provide CSI feedback to the base station would be much larger than in conventional systems.

The aforementioned issues can be resolved by operating in the time-division duplex (TDD) mode and take advantage of the reciprocity between the uplink and the downlink channels during the coherence time interval of the channel. However, frequency-division duplex (FDD) may be applicable in particular cases where the number of terminals and base station antennas is small. (Larsson et al. 2014.)

As stated by Ashikhmin & Marzetta (2012) and shown in figure 4, each coherence interval in a TDD scheme comprises of four phases;

1. The uplink phase: Each terminal transmits data to its assigned base station.
2. All the terminals synchronously transmit pilot sequences of length τ.
3. The base stations use the received pilot signals to estimate the channel vectors and use these estimates to decode the previously received data signals by the use of maximum ratio combining (MRC).
4. The downlink phase: The channel vector estimates are then used to compute the beamforming weights that are used for the directed downlink transmission of data to the terminals.

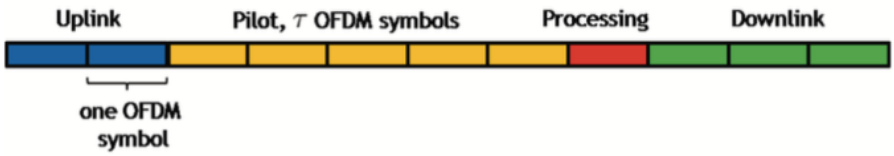

Figure 4. Coherence interval of TDD scheme (Ashikhmin & Marzetta 2012)

2.2. Precoding

The multipath propagation in a radio channel results in the received signal to comprise of a superposition of several delayed and scaled replicas of the transmitted signal. When the signal bandwidth is larger than the coherence bandwidth, the signal undergoes frequency-selective fading. At the receiver, intersymbol interference (ISI) is experienced leading to an increase in BER and in turn degrading the performance of the

communication system. ISI is a major problem for communication systems with high data rates such as with MIMO. One of the solutions to mitigate the detrimental effect of ISI is the use of equalizers at the receiver. The equalizer ideally filters the received signal to eliminate the channel distortions, namely, ISI and multiuser/multi-antenna interference as well as noise. However, the equalization process can be complex. In order to simplify its complexity, the transmitter obtains the CSI and uses it to perform precoding on the data streams before transmission. These precoded data streams allow for a simpler equalizer design at the receiver. (Chellapa & Sergios 2013.)

As described by Chockalingam & Rajan (2013), precoding is the process of encoding the information signals using CSI at the transmitter. The transmitter uses the CSI to encode the information symbols into transmit vectors. The optimal transmission scheme is based on a concept known as dirty paper coding (DPC), where the transmitter encodes the information symbols for all users using perfect knowledge of CSI. With this perfect knowledge of the CSI for all users, the transmitter can compute the interference and deduct it prior to transmission. This leads to the system performing as though the interference from other user data streams was not present. However, the DPC based transmission scheme is too complex for practical implementation. Therefore, more practical precoding techniques are implemented which fall under one of two categories, namely, linear precoding and non-linear precoding.

2.2.1 Linear precoding

With linear precoding, the information symbols are linearly transformed using a precoding matrix. Mathematically, it can be represented as follows:

$$\mathbf{x} = \mathbf{T}\mathbf{u} \tag{1}$$

Where $\mathbf{x}$ is the transmit vector, $\mathbf{u}$ is the information symbol vector and $\mathbf{T}$ is the precoding matrix. The precoding matrix is chosen based on the available CSI at the transmitter (CSIT).

2.2.2 Non-linear precoding

Non-linear precoding techniques are relatively more complex compared to linear precoding techniques, which is not desired for large multi-user systems. However, they achieve a relatively higher performance, particularly when the number of serviced users is small. The increased performance of non-linear precoding techniques is due to the additional operations like interference pre-subtraction and optimal user ordering.

2.3. Multi-antenna wireless channels

As explained by Chockalingam & Rajan (2013), multi-antenna wireless channels are broadly categorized into two groups, point-to-point and multi-user channels. One of the defining attributes of a wireless channel is the fluctuation of the channel strength with respect to time and frequency. These fluctuations are classified into two:

i. Large scale fading: This arises due to path loss caused by long transmission distances and shadowing by large objects like buildings and trees, to mention a few. Large scale fading is frequency independent.
ii. Small scale fading: This arises due to the constructive and destructive interferences of the multiple signals that are caused by multipath propagation between the transmitter and receiver. Small scale fading is frequency dependent.

Furthermore, small scale fading is further broken down into two categories:

i. Frequency selective channel: This occurs when the signal bandwidth is larger than the coherence bandwidth of the channel. This occurrence leads to intersymbol interference.
ii. Frequency-flat (or flat fading) channel: This is the inverse of the frequency selective channel. It occurs when the signal bandwidth is much smaller than the coherence bandwidth of the channel. A frequency-flat channel does not cause severe ISI and hence it is the desired type of channel. Fortunately, there exists a

technique that converts a frequency selective channel into multiple parallel frequency-flat channels. This technique is known as orthogonal frequency division multiplexing (OFDM).

In terms of channel fluctuation with respect to time, the wireless channels are further classified as slow fading or fast fading. In a wireless communications system, CSI is constantly being estimated due to the channel's varying nature as well as the mobility of the users. The fading rate of the channel in relation to the rate of CSI estimation (or signaling rate) determines a slow fading and fast fading channel. A slow fading (or time-flat) channel is one in which the signaling rate is faster than the fading rate of the channel. Meaning, the channel state is constant during the time interval between one CSI estimate and the next. On the other hand, a fast fading (or time-selective) channel is one in which the signaling rate is slower than the fading rate of the channel. This means that by the time data transmission is carried out using the currently obtained CSI, the channel state would have already changed hence leading to signal detection errors at the receiver.

Multi-antenna wireless channels with t transmit antennas and r receive antennas are modeled as a linear channel with an equivalent baseband r×t channel matrix, **H**.

$$\mathbf{H} = \begin{bmatrix} \mathrm{h}_{11} & \cdots & \mathrm{h}_{1\mathrm{t}} \\ \vdots & \ddots & \vdots \\ \mathrm{h}_{\mathrm{r}1} & \cdots & \mathrm{h}_{\mathrm{rt}} \end{bmatrix} \tag{2}$$

To elaborate the matrix in equation (2), h_{ij} is the channel impulse response (or fading coefficient) between the i^{th} receiver and j^{th} transmitter. The average channel gain between the i^{th} receiver and j^{th} transmitter is $g_{ij} = E[|h_{ij}|^2]$. These channel gains are also referred to as CSI.

2.4. Pilot Contamination

In the earlier sub-chapters, the importance of CSI knowledge (or channel gains) has been clearly indicated. Chockalingam & Rajan (2013) state, “In practice, these gains are estimated at the receiver, either blindly/semi-blindly or through pilot transmissions (training).” They continue by elaborating that in FDD systems, channel gains are estimated at the receiver and then fed back to the transmitter for precoding purposes. This scheme requires relatively more resources due to the feedback process. In TDD systems, where channel reciprocity holds, the transmitter can estimate the channel from the received pilots from the user equipments, and use it for precoding. This scheme requires fewer resources and is suitable for large networks with a large array of base station antennas.

As mentioned before, TDD mode is the optimal mode of operation for massive MIMO due to the magnitude of transmission links. Hence, in this case, channel state estimation is performed through pilot transmissions as describe in the previous paragraph. Prior to data transmission, each UE in a massive MIMO system is ideally allocated an orthogonal uplink training sequence (also known as pilot signals). However, the maximum number of orthogonal training sequences that can exist is limited by the ratio of the coherence time of the channel to the channel delay spread. Hence, in multicellular systems, the available supply of these orthogonal training sequences is easily exhausted. (Larsson et al. 2014.)

In order to simultaneously cater to a large number of UE, pilot reuse policy is implemented. UE in the neighboring cells reuse these limited orthogonal training sequences at a specific reuse factor as shown in figure 5. The effect and, ultimately, negative consequence that arises due to pilot reuse is termed pilot contamination. When the base station receives a pilot signal from a UE, it uses the received signal to estimate the CSI that turns out to be contaminated by the pilot signals from other terminals that share the same training sequence. Hence, using this corrupted CSI for downlink transmission of data results in transmission errors. This in turn results in drastic degradation of the system by limiting the benefits of massive MIMO and that is why it

is of great importance to establish techniques to mitigate this effect. (Larsson et al. 2014.)

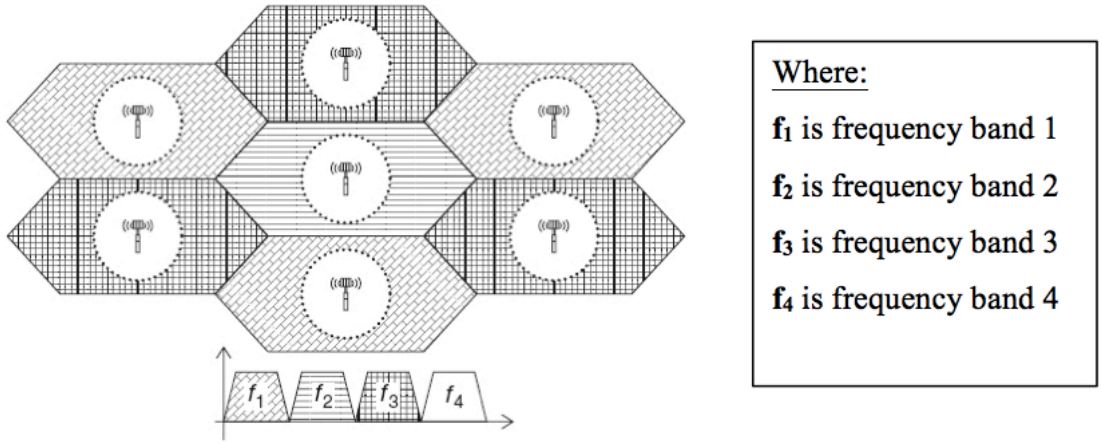

Figure 5. Fractional reuse factor (Taha, Ali & Hassanein 2012).

However, it is important to note that non-orthogonal training sequences are not the only source of PiC. Practically, other sources of PiC could be hardware impairments (due to distortions that interfere with the pilot signals) and non-reciprocal transceivers. (Elijah, Leow, Rahman, Nunoo & Iliya 2015a.)

Based on literature, Larsson et al. (2014) state three approaches to mitigate PiC:

1. Optimizing the allocation of pilot waveforms. One way to achieve this is by reducing the frequency reuse factor for the pilots (but not necessarily for the actual data i.e. payload). This allows for cells that share the same pilot sequence to be further apart hence reduced interference.
2. The use of smart channel estimation algorithms or even blind techniques that eliminate the need for pilots altogether.
3. The development of new precoding techniques that take the network structure into account.

Approach number 3 is the main focus of this thesis. The following sub-chapter highlights the various works on precoding schemes that mitigate PiC.

2.5. Research on precoding techniques for mitigation of pilot contamination

As the number of base station antennas, M, increases with no bound, the effects of additive noise at the receiver, intra-cell interference as well as fast fading disappear. The sole challenge that remains is the inter-cell interference that causes PiC. In the absence of PiC, signal-to-interference-plus-noise ratio (SINR) scales linearly with M and does not saturate as M tends to infinity. On the other hand, the presence of PiC results in SINR saturation due to the corruption of channel estimates caused by interfering users. (Elijah, Leow, Tharek, Nunoo & Iliya 2015b.)

The following reviewed literatures are based on the multi-cell TDD-based massive MIMO OFDM systems that implement pilot training for CSI estimation.

One of the precoding techniques to mitigate PiC, which was proposed by Jose, Ashikhmin, Marzetta & Vishwanath (2011), is multi-cell MMSE-based precoding. MMSE stands for minimum mean squared error. This technique does not require any coordination between base stations and it explicitly takes into account the set of training sequences allocated to the UE. The authors state that since PiC originates from the use of non-orthogonal training sequences, the key point is to account for the allocation of the training sequences in the precoding design. This approach is not very common and instead, the designed precoding methods take into account the inter-cell interference and not the ultimate source itself (the non-orthogonal training sequences). The performance of the proposed precoding scheme was compared to the performance of single-cell precoding schemes such as zero forcing with the performance metric being sum rate (the total system throughput). It was indicated that the presence of PiC leads to the saturation of achievable rates by the users when increasing the number of base station antennas. Multi-cell MMSE-based precoding outperformed the single-cell precoding

schemes and it proved suitable for maximizing the minimum of the rates achieved by all the users.

Another contribution is pilot contamination precoding (PCP) that was proposed by Ashikhmin & Marzetta (2012). Unlike multi-cell MMSE-based precoding, PCP employs the use of limited collaboration between base stations in the network by the use of a network hub. The network hub is responsible for computing the PCP precoding matrices. The results showed that inter-cell interferences as well as noise vanishes as the number of base station antennas, M, tends to infinity. Therefore, SINR tends to infinity as M tends to infinity. However, practically, massive MIMO systems have base stations with a finite number of antennas. In this case, PCP does not work well in resolving the issue of inter-cell interferences. Consequently, Ashikhmin, Marzetta & Li (2014) further developed and renamed PCP to Large-Scale Fading Precoding (LSFP) due to the fact that LSFP better reflects the idea of the PCP protocol. The analysis of the performance of PCP on the mitigation of inter-cell interference revealed that, for a finite number of base station antennas, there exist some other consequences of inter-cell interference other than PiC which LSFP successfully eliminates. For better performance of the LSFP, the authors suggested that the system should be designed with a frequency and pilot reuse factor higher than one. However, this leads to longer training sequences which in turn lead to longer training time and consequently a relatively slower system.

In addition to LSFP, Neumann, Joham & Utschick (2015) proposed the channel distribution information (CDI) precoding. CDI precoding was developed as an extension of PCP where an additional precoding stage is added that is independent of the instantaneous CSI. However, the additional stage depends solely on the channel distribution information. Achievable rates are known to only depend on the statistics of the channel i.e. CDI. This is the motivation behind the CDI-based linear precoding proposed by the authors. For the ease of simulation, the authors focused on a simple zero-forcing approach. The results revealed that, similar to PCP, CDI zero-forcing needs a very large number of antennas to significantly outperform the alternatives. However, CDI zero-forcing produced much higher spectral efficiency per user in comparison to PCP zero-forcing. It was proved that CDI precoding completely

suppresses the interference that causes PiC leading to a significant gain in spectral efficiency in massive MIMO systems affected by PiC.

Another precoding technique named beamforming training and pilot contamination precoding (BT-PCP) was proposed by Zuo, Zhang, Yuen, Jiang & Luo (2015). This precoding scheme also employs limited collaboration between base stations to share transmit signals. Unlike with PCP and LSFP, the performance metric used for BT-PCP is spectral efficiency. BT-PCP proved to achieve higher spectral efficiency than PCP in the practical scenario in which the number of base station antennas was finitely large. It also proved to perform quite close to the perfect CSI scenario where PiC is not a factor. As it has been seen mentioned before, CSI at the base station is essential for uplink detection and downlink precoding. So far, CSI at the user side has not been highlighted in massive MIMO due to the use of TDD scheme where CSI is only known at the base station. However, the system performance can be enhanced when the users have knowledge of the downlink CSI, which can be achieved through beamforming training. This is the key element of BT-PCP. As discussed in the earlier sub-chapters, the conventional downlink communication of the TDD protocol consists of the uplink training phase and the downlink data transmission phase. With beamforming training there exists an additional phase where the effective channel is estimated by the users through the downlink pilots from the base stations. Beamforming training is what contributes to the high performance of BT-PCP. However, the authors suggested that for further improvements the correlation of the channel should be taken into consideration since their analysis only focused on uncorrelated channels due the mathematical complexities behind channel correlation.

Concurrently, Liu, Cheng & Yuan (2015) proposed a technique that employed a novel uplink training scheme in conjunction with a downlink pilot contamination elimination precoding (PCEP) scheme. This proposed scheme was motivated by the works of Ashikhmin, Marzetta & Li (2014). The novel uplink training scheme proposed confines PiC to be within each cell rather than between neighboring cells. This is very different from the cases previously discussed. The proposed uplink training scheme is cell-specific. This means that the users in one cell adopt the same training sequence which is

orthogonal to the one adopted by users in the neighboring cells. Hence, within the cells, the pilots are non-orthogonal which is contrary to the conventional pilot allocation, which is user-specific (meaning the pilots within the cell are orthogonal). Since the number of neighboring cells is much smaller than the number of users that can be simultaneously served in one cell, the length of training sequences is significantly reduced in the proposed cell-specific training scheme. This leads to higher spectral efficiency. The PCEP matrices are computed locally at each base station since the precoding scheme only deals with intra-cell interference hence no collaboration is required between base stations. This reduces signaling overhead. As a result, the proposed scheme exhibited a very high performance compared to the user-specific schemes (such as LSFP) in terms of average sum rate achieved by the users.

Finally, Xu, Wang & Wang (2015) proposed the joint use of the H-infinity (H-inf) criterion on channel estimation (CE) and precoding schemes for mitigation of PiC. The authors pointed out that existing research generally address CE and precoding separately. However, since CE is a fundamental part of precoding, it is important to consider them jointly to mitigate the impact of PiC. In the uplink phase, the idea of the H-inf criterion is to find a CE method with which the ratio between the CE error and the input noise/interference is less than a prescribed threshold. Whereas in the downlink phase, the idea of H-inf precoding is to find the CE based precoding matrix whose ratio between the precoding error and the noise/interference from other cells is less than a prescribed positive threshold. The performance metric used was the downlink achievable rate. Comparison was made between combinations of H-inf precoding methods, zero-forcing and MMSE (for the downlink phase) with H-inf CE methods and MMSE (for the uplink phase). Numerical results revealed that joint use of the H-inf criterion in CE and precoding present significant rate gains compared to many popular combinations of CE and precoding. The results also showed that the performance of the precoding depends only on the uplink thresholds of the H-inf CE.

3. SYSTEM MODEL AND SIMULATION

3.1. System Model

The software used to build the system is a MathWorks product known as MATLAB, short for Matrix Laboratory. It is a powerful tool used to design and analyze systems and products by the use of matrix-based MATLAB language.

3.1.1 Network Setup

The implemented system model is a multi-user multi-cellular network with Rayleigh fading channels. The system model consists of a center cell (the desired cell) surrounded by six co-channel cells in the first tier whose centers are at a distance *D* from the center of the desired cell. *D* is the reuse distance and is equated as;

$$\mathrm{D} = \mathrm{R}\sqrt{3\mathrm{N}} \tag{3}$$

Where, *R* is the cell radius and *N* is the cluster size. Each cell has a single base station (BS) consisting of *M* omnidirectional antennas that are horizontally aligned. All base stations are placed at the center of the cell. In each cell, *K*=8 UE can be served simultaneously. The number of UE remains fixed during the system analysis. For analysis of the worst case scenario, the UE in the desired cell are randomly placed on the cell edges whereas the UE in the co-channel cells are randomly scattered within the cell as shown in figure 6. For simplicity, in the simulation process the cells are assumed to be circular.

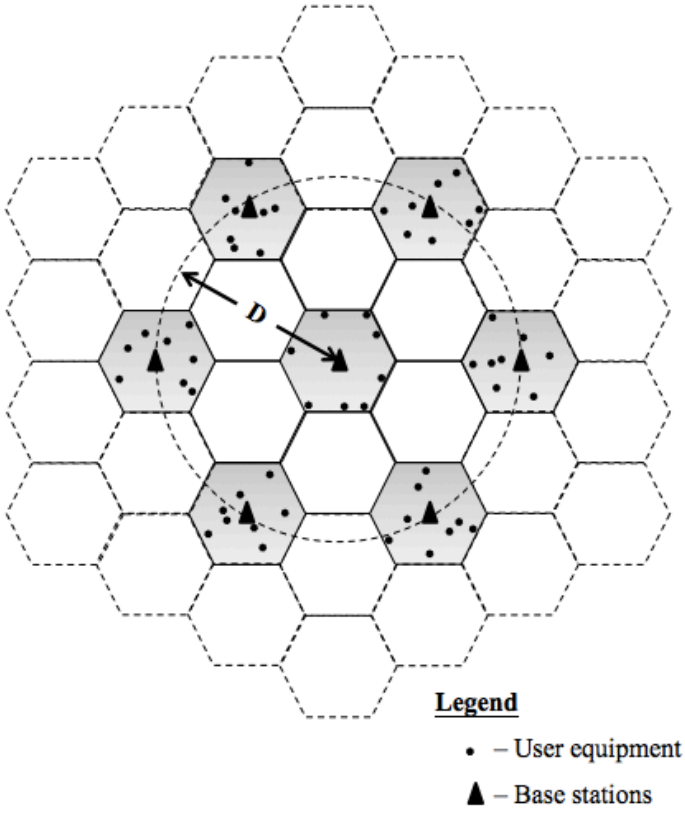

Figure 6. Aerial view of the cellular network (cluster size = 3).

3.1.2 Channel Model

As mentioned earlier, the channel is a Rayleigh fading channel. The channel is modeled based on the concept of adaptive transmit beamforming. Transmit beamforming is in fact the essence of precoding. As stated by Björnson, Bengtsson & Ottersten (2014), transmit beamforming increases spectral and energy efficiency since it allows for the transmit antenna array to focus the signal energy in the direction of the desired user with relatively very low signal energy directed towards the undesired users. The ideal case is not to have any signal energy directed towards the undesired users but, practically, this is not the case due to limited spatial directivity of finite transmit antennas. With

transmit beamforming, *K* spatially separated users are served simultaneously through space-division multiple access (SDMA). Figure 7 illustrates this concept.

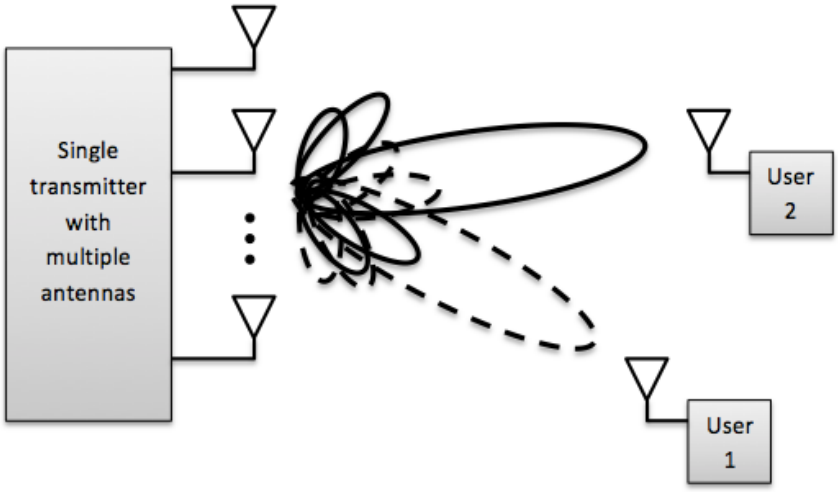

Figure 7. Adaptive transmit beamforming.

The channel modeling procedures are as follows:

1. The steering vector for each user, $\mathbf{a}_k(\theta_k, \phi_k)$, is given by;

$$\mathbf{a}_k(\theta_k, \phi_k) = \left[1 \quad \exp\left(-j\Delta\Psi_2(\theta_k, \phi_k)\right) \quad \ldots \quad \exp\left(-j\Delta\Psi_M(\theta_k, \phi_k)\right)\right]' \qquad (4)$$

Where, θ_k and ϕ_k are the elevation and azimuth angle of the plane wave from the k^{th} user, respectively. $\Delta\Psi_M$ is the phase difference between the signal received at BS antenna element *M* and the reference antenna element.

$$\Delta\Psi_M = \beta(x_m \cos(\phi_k)\sin(\theta_k) + y_m \sin(\phi_k)\sin(\theta_k) + z_m \cos(\theta_k)) \qquad (5)$$

Where, $\beta = {}^{2\pi}/_{\lambda}$ is the phase propagation factor, λ is the wavelength of the received signal and (x_m, y_m, z_m) is the Cartesian position of the BS antenna element *m* with respect to the reference antenna element.

2. The channel impulse response vectors for each user, are then computed using equation (6) below.

$$\mathbf{h}_k = \frac{\alpha_k}{d_k^{\,2}} \times \mathbf{a}_k(\theta_k, \phi_k) \tag{6}$$

α_k is a complex magnitude of the channel fading coefficient between the BS and user *k* and d_k is the distance between the BS and user *k*. α_k is Rayleigh distributed and each user experiences an independent attenuation coefficient.

3. The collective channel response matrix, **H**, between the BS antenna elements and the randomly scattered users is a concatenation of the individual channel response vectors for each user.

$$\mathbf{H} = [\mathbf{h}_1 \quad \mathbf{h}_2 \quad \ldots \quad \mathbf{h}_K] \tag{7}$$

H is an *M* x *K* matrix.

The network simulation is divided into two phases, the uplink phase and the downlink phase.

3.1.3 Uplink phase

As discussed in the literature review, channel estimation is performed in the uplink phase by the use of orthogonal training sequences that are known at the BS. The users in the center cell are assigned a set of orthogonal training sequences, of length $l = 2\text{^}n$ ($n \in Z^+$), which are re-used by the co-channel cells around it (pilot reuse). This pilot reuse leads to PiC during the channel estimation process. For simplicity, the channel

estimation technique implemented is based on least squares (LS). The LS channel estimator, also known as a zero-forcing estimator, is a simple traditional Gaussian assumption channel estimator (Bhatia, Mulgrew & Falconer 2007).

During the uplink phase, each user transmits its assigned pilot which is received by the BS antenna array as shown in equation 8 below.

$$\mathbf{Y}_k = \mathbf{h}_k \mathbf{x}_k + \mathbf{N} \tag{8}$$

Where $\mathbf{Y}_k$ is the M x l received signal from the k^{th} user, $\mathbf{h}_k$ is the M x 1 channel impulse response between the k^{th} user and the BS antenna array, $\mathbf{x}_k$ is the pilot signal from the k^{th} user and $\mathbf{N}$ is the M x l additive white Gaussian noise (AWGN) at the receiver (BS antenna array).

The channel is estimated using the equation 9 below.

$$\widehat{\mathbf{H}} = \mathbf{Y}\mathbf{X}^{-1} \tag{9}$$

Where $\widehat{\mathbf{H}}$ is the M x T channel estimate, $\mathbf{Y}$ is the M x l sum of received signals at the BS antenna array from all the users in the cell i.e. $\mathbf{Y} = \sum_K \mathbf{Y}_k$. Finally, $\mathbf{X}$ is the T x l training symbol matrix containing the training sequences assigned to all users.

In the presence of inter-cell interference, the BS in the desired cell receives pilot signals from all users in the surrounding co-channel cells as $\mathbf{Y} = \sum_c \mathbf{Y}_n$. Where C is the total number of co-channel cells (in this case $C = 6$) and $\boldsymbol{Y}_n$ is the sum of the received signals from the n^{th} co-channel cell. This causes PiC. Therefore, the corrupted channel estimate equated as;

$$\widehat{\mathbf{H}}_{\mathbf{corrupted}} = \sum_c \mathbf{Y}_n \mathbf{X}^{-1} \tag{10}$$

3.1.4 Downlink phase

The precoding process takes place in the downlink phase. The BS uses the estimated channels to produce beamforming weights that are used to direct the payload to the desired user. As discussed in the literature review, various precoding techniques could be implemented that vary in complexity and efficiency. For simplicity, zero-forcing (ZF) precoder is employed in this work.

With ZF, the beamforming weights are computed as follows;

$$\mathbf{W}_{\mathrm{ZF}} = \widehat{\mathbf{H}}^{\mathrm{H}}(\widehat{\mathbf{H}}\widehat{\mathbf{H}}^{\mathrm{H}})^{-\mathbf{1}} \tag{11}$$

Where, $\mathbf{W}_{\mathrm{ZF}} = [\mathbf{w}_1, \mathbf{w}_2, \ \ldots \ \mathbf{w}_{\mathrm{K}}]$; $\mathbf{w}_{\mathrm{K}}$ is the ZF beamforming weight of the K^{th} user. The ZF beamforming weights are simply the pseudo-inverse of the channel impulse responses. The beamforming weights are such that they eliminate inter-user (also known as intra-cell) interference i.e. $\mathbf{h}_{\mathrm{i}}^{\mathrm{H}}\mathbf{w}_{\mathrm{k}} = 0$ for $i \neq k$ while $\mathbf{h}_{\mathrm{i}}^{\mathrm{H}}\mathbf{w}_{\mathrm{i}} = 1$, in perfect CSIT conditions.

The transmitted signal from the BS to the users after beamforming is;

$$\mathbf{u} = \sum\nolimits_{\mathrm{K}} \mathbf{w}_{\mathrm{k}}\mathbf{s}_{\mathrm{k}} \tag{12}$$

Where $\mathbf{s}_{\mathrm{k}}$ is the payload for the k^{th} user. The signal received by each user in the cell then becomes;

$$\mathbf{y}_{\mathrm{k}} = \mathbf{h}_{\mathrm{k}}^{\mathrm{H}}\mathbf{u} + \mathbf{n}_{\mathrm{k}} \tag{13}$$

3.2. Simulation

In this work, Monte Carlo simulations are implemented to estimate the value of a parameter. As stated by Kosbar, Tranter, Rappaport & Shanmugan (2003), in Monte Carlo simulations, the value of the parameter is estimated by running the underlying stochastic experiment multiple times. The number of repetitions should be as large as possible for a better estimate.

The simulation is designed in different ways based on the performance metric. Three performance metrics are used, namely, probability of outage, average achievable sum capacity and bit error rate (BER). Probability of outage is the probability that the SINR at the receiver is below a certain threshold, hence leading to outage. The achievable sum capacity is the sum of the average capacity achieved by each serviced user in the cell. Lastly, BER is the probability of receiving a bit in error.

In order to study the effect of PiC on the mentioned performance metrics, the network is analyzed in two scenarios; one in which the CSIT is corrupted by the pilot signals from the UE in the co-channel cells and the other in which there is no presence of PiC. Furthermore, the effect of PiC is studied in the worst-case scenario where the UE in the desired cell are on the edges of the cell.

In the simulation, the probability of outage is given by;

$$P_{outage} = P(SINR_{achieved} < SINR_{threshold}) = \frac{\text{number of outages}}{\text{number of repetitions}} \tag{14}$$

The SINR achieved by each user, *k*, is given by;

$$SINR_k = \frac{P \times \left|\mathbf{h}_k^H \mathbf{w}_k\right|^2}{\sum_{j \neq k}\left(P \times \left|\mathbf{h}_k^H \mathbf{w}_j\right|^2\right) + \sigma_n^2} \tag{15}$$

Where, P is the BS transmit power and σ_n^2 is the noise power at the receiver.

The capacity achieved by each user, *k*, is given by;

$$C_k = \log_2(1 + SINR_k) \tag{16}$$

Finally, the BER is computed using equation (17) below under the assumption that the modulation scheme used is 16-QAM (16-ary quadrature amplitude modulation).

$$BER_k = {}^{3}/_{4}\, Q\left(\sqrt{{SINR_k}/{5}}\right) \tag{17}$$

Figures 8 and 9 illustrate the simulation flowcharts to measure the probability of outage, the average achievable sum capacity and the BER.

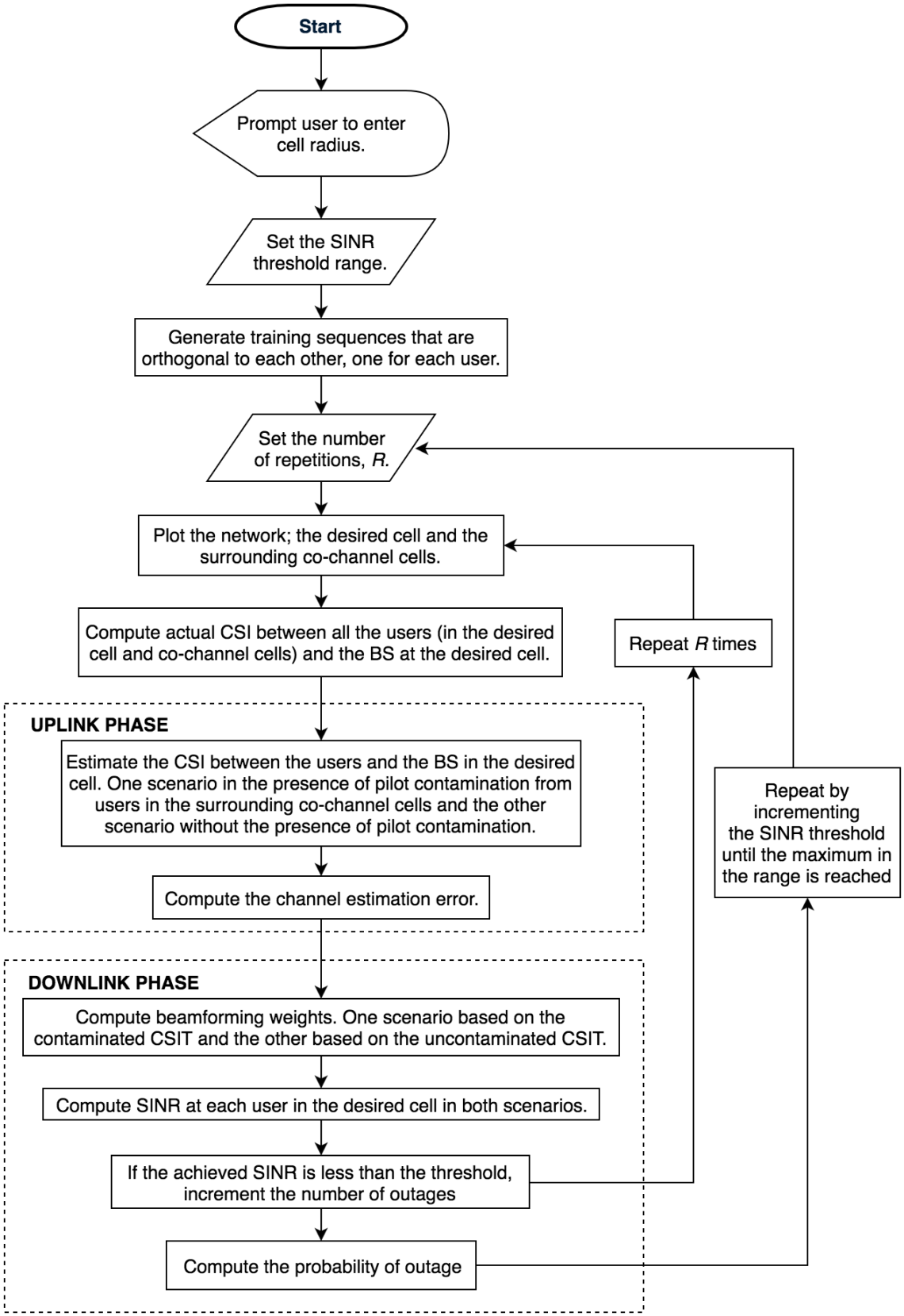

Figure 8. Simulation flowchart for the probability of outage.

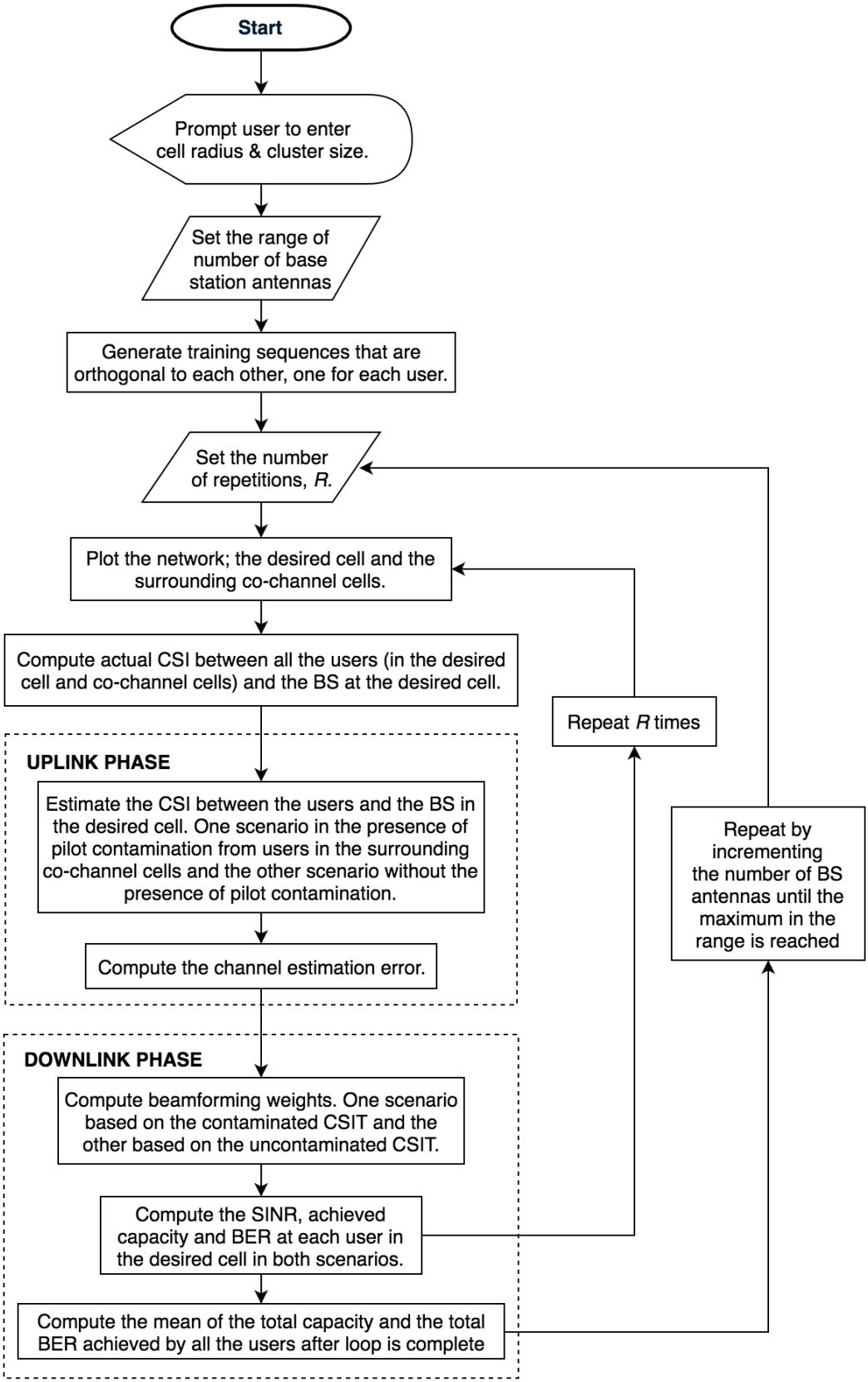

Figure 9. Simulation flowchart for the average achievable sum capacity and BER.

4. DISCUSSION AND CONCLUSIONS

4.1. Simulation results

Table 1 consists of the network parameters for the simulation.

Table 1. Network parameters.

Parameter	Value
Height of base station	300m
Number of users per cell	8
Length of training sequence	8
Carrier frequency	3.7GHz
Normalized antenna separation	$3/\pi$
Noise power at BS	-80dBm
Noise power at user terminal	-100dBm
Base station transmit power per antenna	0dBW
Cell radius	500m

4.1.1 Channel estimation error

To analyze the effect of PiC on the channel estimation, the normalized mean square error (NMSE) of the estimate is computed. NMSE is a measure of how accurate the channel estimation is. It is computed using equation 18 below.

$$\mathrm{NMSE} = \frac{\mathrm{E}\left[\left|\mathbf{H} - \widehat{\mathbf{H}}\right|^2\right]}{\mathrm{E}[|\mathbf{H}|^2]} \tag{18}$$

Where, $\mathbf{H}$ is the actual channel and $\widehat{\mathbf{H}}$ is the estimated channel. The lower the NMSE value, the more accurate the channel estimation is.

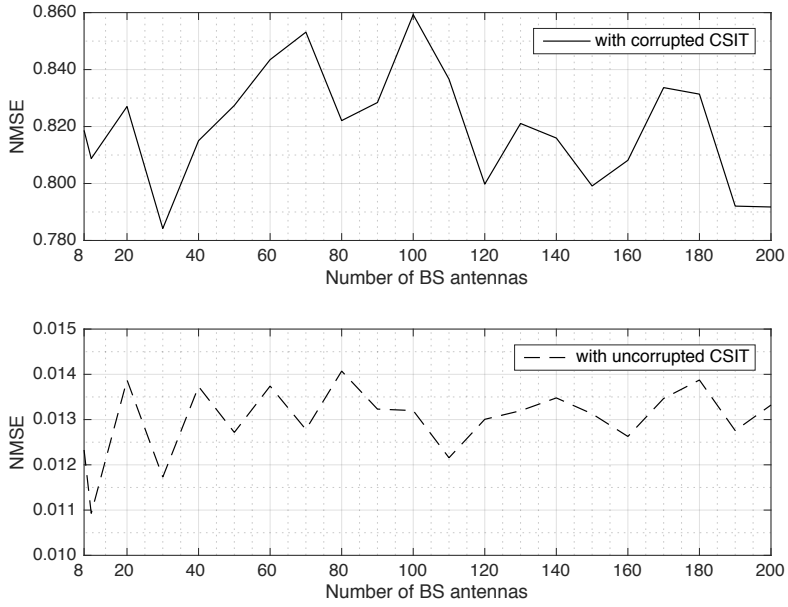

Figure 10. Normalized mean square error of the channel estimation.

In figure 10, the cluster size is one. Additionally, the term *corrupted CSIT* means CSIT in the presence of PiC and the term *uncorrupted CSIT* means CSIT in the absence of PiC. From the figure, it is seen that the NMSE values vary between 0.78 and 0.86 with corrupted CSIT while with uncorrupted CSIT they vary between 0.01 and 0.015. The fluctuations in the NMSE with increasing number of BS antennas are due to the randomness of the channel and the random locations of the UE. Conclusively, the NMSE values clearly show that PiC leads to significantly larger channel estimation errors.

4.1.2 Probability of outage

Figure 11 illustrates how PiC affects the probability of outage at varying cluster sizes when the number of BS antennas is fixed at 20. In all the subplots, the x-axes represent

the SINR threshold in decibels (dB) and the y-axes represent the average probability of outage in percentage (%).

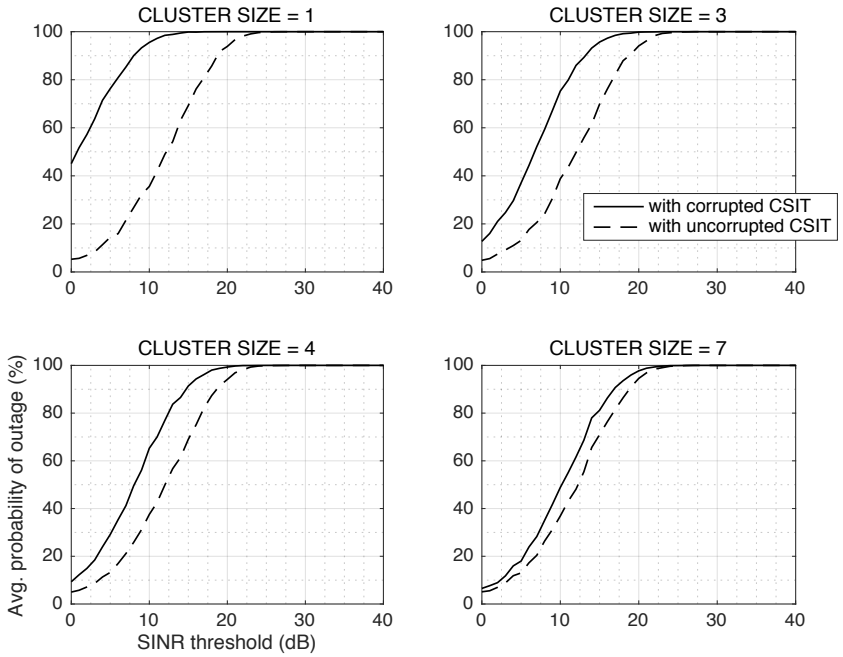

Figure 11. Probability of outage in the presence vs. in the absence of PiC with increasing cluster sizes.

The probability of the edge users being in outage appears to be higher in the presence of PiC. This is justified by the fact that the achieved SINR at the UE is lower under corrupted CSIT as shown in figure 12. The reduction in SINR is due to the fact that the beamforming weights computed from the corrupted CSIT do not significantly eliminate the intra-cell interferences. However, as the cluster size increases, the effect of PiC disappears, as expected, since the co-channel cells are further away from the desired cell. Due to free space path losses (FSPL), the power of the pilot signals from the co-channel cells decays in proportion to the fourth power of the distance between the transmitter and receiver i.e. $P_r \propto \frac{1}{d^4}$. Where, P_r is power received at distance *d* from the transmitter.

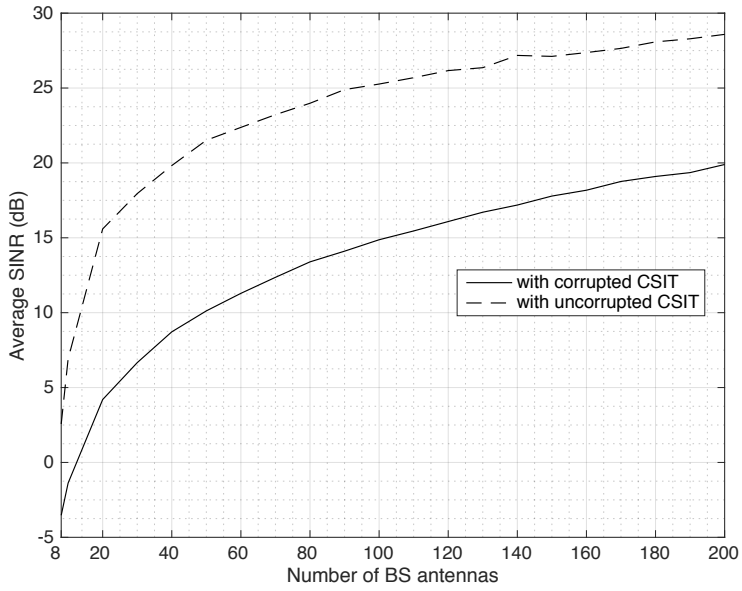

Figure 12. SINR achieved in the presence vs. in the absence of PiC.

Figure 13 clearly shows how increasing the cluster size alone improves the performance of the network (in terms of outage) in the presence of PiC when the number of BS antennas is fixed at 20. However, increasing the cluster size requires more orthogonal sets of orthogonal pilots, one set for each cell in the cluster. As mentioned in the earlier chapters, the number of orthogonal pilots is directly proportional to the length of the pilot, which is limited by the coherence time of the channel. Due to this, the number of orthogonal pilots and in turn the cluster size is limited. Having seen the effect of the cluster size on the strength of the PiC, the simulations to follow will be analyzed only in the case where the cluster size is one in order to study its full effect.

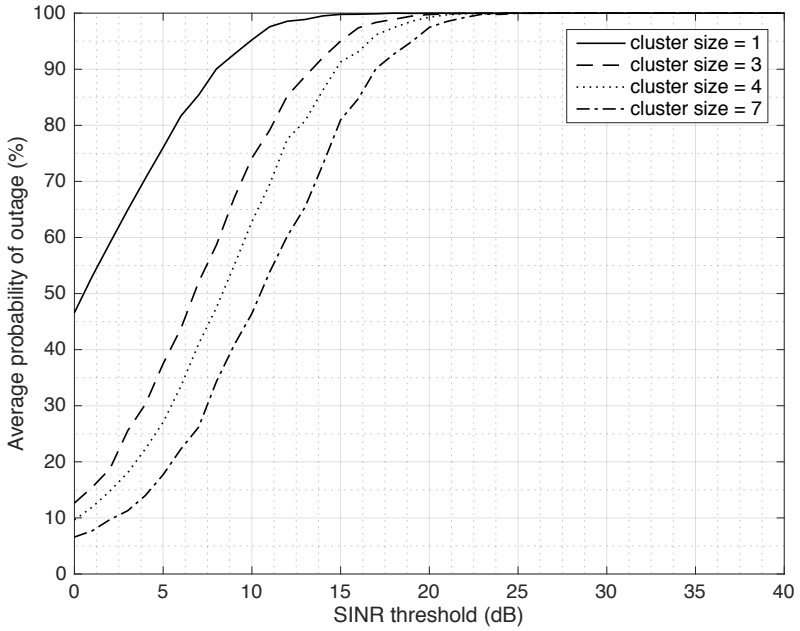

Figure 13. Probability of outage with increasing cluster size in the presence of PiC.

In conjunction with increasing the cluster size, increasing the number of antennas at the BS also significantly lowers the probability of a user being in outage as shown in figure 14. It is observed that as the number of antennas at the BS is tripled, the probability of outage decays exponentially. This improvement is due to a concept known as diversity order, which is a measure of the diversity gain. The diversity order of a system indicates the number of independently fading channels between the transmitter and the receiver due to transmit diversity, in this case. If the channel responses between all the users are completely uncorrelated, the diversity order is equal to the number of transmit antennas, in the case of a MISO system. The higher the diversity order, the lower the chances of a user being in outage. This is because it is less likely for all the channels to be in deep fade at the same time.

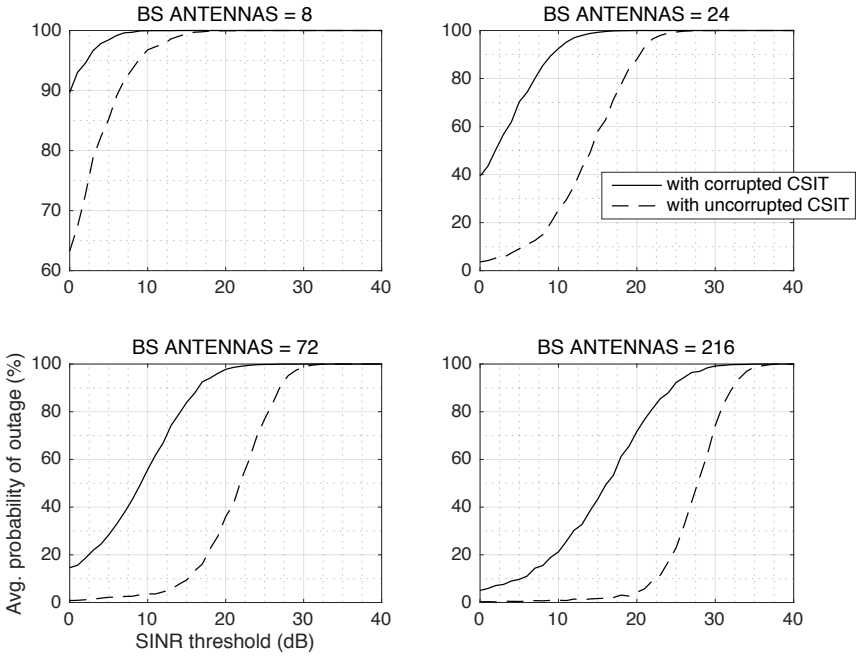

Figure 14. Probability of outage in the presence vs. in the absence of PiC with increasing BS antennas.

It can be further observed in figure 14 that increasing the number of BS antennas, improves the performance of the system but does not eliminate the effect of PiC. In fact, the effect of PiC is more prominent at the high SINR region as the number of BS antennas increases as shown in figure 15. In the figure, the term *probability of outage ratio* is the ratio of the probability of outage (at a particular SINR threshold) under corrupted CSIT over the probability of outage (at the same SINR threshold) under uncorrupted CSIT. Since the probability of outage under corrupted CSIT is larger, a probability of outage ratio greater than one is produced meaning there is an increase in the probability of outage. The probability of outage ratio is highest when the BS antenna array is large at which a bigger range of SINR threshold levels is affected. For instance, when the SINR threshold is 20dB and the number of BS antennas is 72, the probability of outage in the presence of PiC is 271.75% of the probability of outage in the absence of PiC. Whereas, when the number of BS antennas is increased to 216, the probability of outage in the presence of PiC is 1682.99% of the probability of outage in the absence of PiC at the same SINR threshold of 20dB. This is a significant difference.

Hence, in massive MIMO systems, PiC significantly limits the UE's performance, in terms of probability of outage, as the BS antenna array grows.

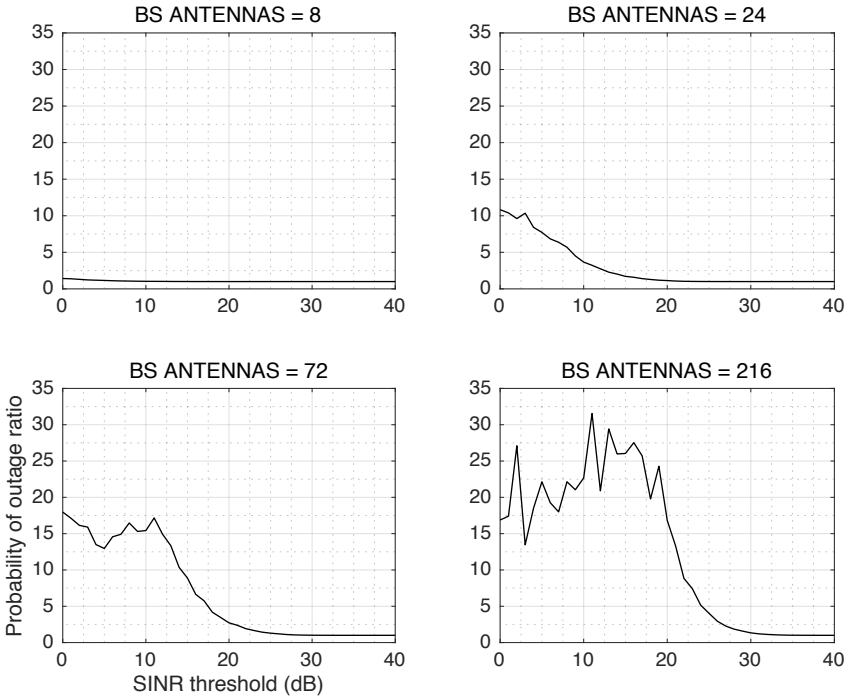

Figure 15. Effect of PiC on the probability of outage.

4.1.3 Average achievable sum capacity

Figure 16 illustrates PiC affects the average sum capacity achieved by the edge users. In the presence of PiC, the sum capacity significantly drops. This can be justified by the fact that the SINR at the UE is negatively affected by PiC as seen in figure 12.

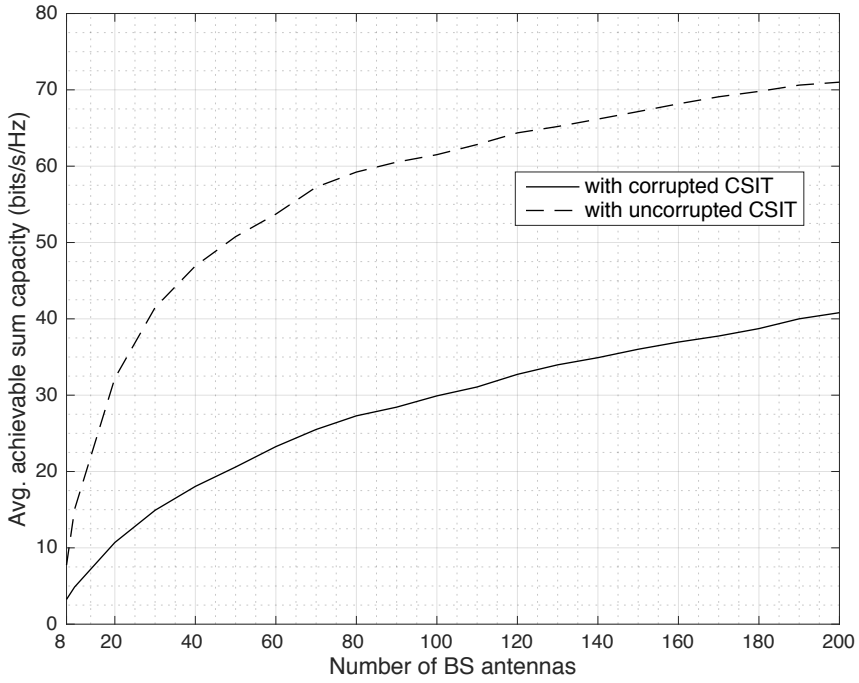

Figure 16. Average sum capacity in the presence vs. in the absence of PiC.

As the number of BS antennas linearly increases, the average sum capacity increases logarithmically. This effect is known as spatial multiplexing gain. Increasing the number of BS antennas/diversity order increases the number of independent channels available for transmission of information to a UE. Therefore, the capacity achieved by a UE increases since it receives more information per transmission. However, the capacity is limited by the degree of freedom of the network, which is the minimum between the number of antennas at the BS and the number of antennas at the UE as shown in equation 19 below.

$$C_k = \min\{M, N\} \times \log_2(1 + SINR_k) \tag{19}$$

Where, *N* is the number of antennas at the UE. Since the UE has a single antenna, increasing the number of antennas at the BS beyond a certain threshold does not significantly increase the multiplexing gain. However, as shown in figure 12, increasing the number of BS antennas leads to a logarithmic growth in the SINR, which explains

the consequent logarithmic growth of the capacity. Figure 17 illustrates how pilot contamination has less of an effect on the sum capacity of the users as the BS antenna array grows. In the figure, *sum capacity ratio* is the ratio of the achievable sum capacity in the presence of PiC over the achievable sum capacity in the absence of PiC. For instance, when the number of antennas at the BS is 80, the average sum capacity in the presence of PiC is 46.25% of the average sum capacity in the absence of PiC. Whereas, when the number of BS antennas is increased to 140, the average sum capacity in the presence of PiC is 52.5% of the average sum capacity in the absence of PiC. However, at this rate of improvement, it would require a very large BS antenna array for the effect of PiC to be eliminated i.e. for the average sum capacity in the presence of PiC to be 100% of the average sum capacity in the absence of PiC.

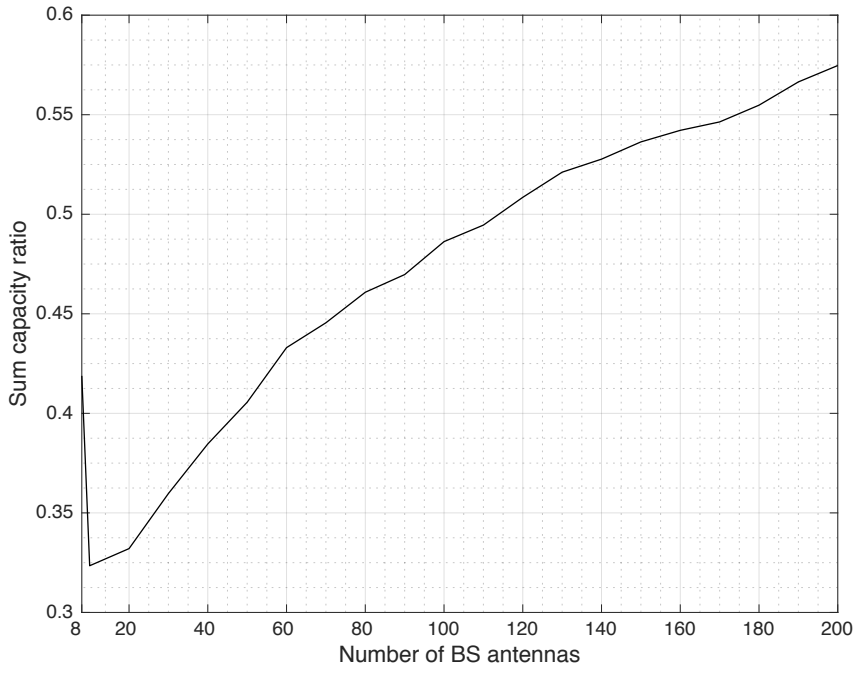

Figure 17. Effect of PiC on the average achievable sum capacity.

4.1.4 Bit error rate

Figure 18 illustrates how PiC affects the BER experienced by the edge users.

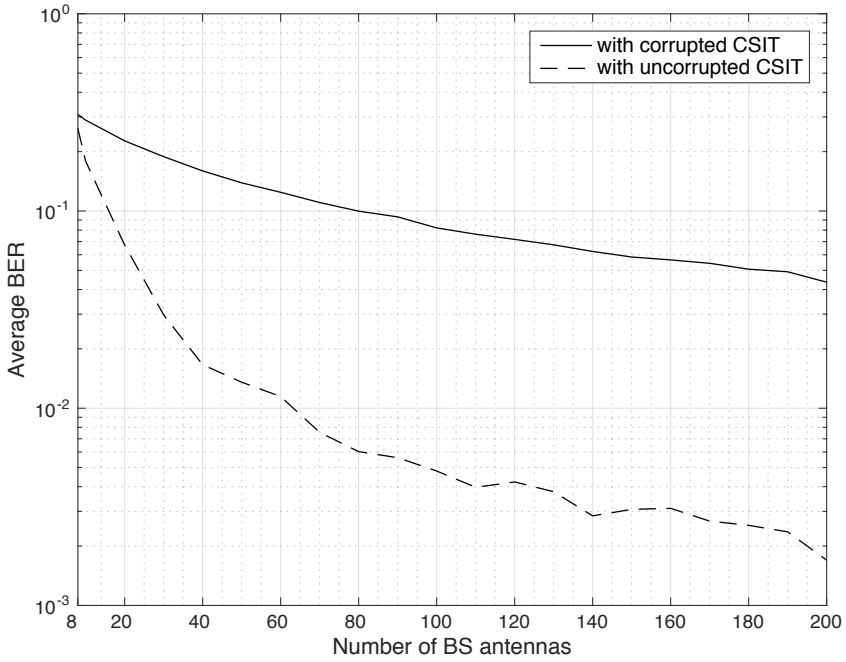

Figure 18. BER in the presence vs. in the absence of PiC.

Just as with the sum capacity, the BER is significantly affected. As the number of BS antennas increases, the BER drops at a much slower rate in the presence of pilot contamination. Bit errors are essentially caused by noise, intra-cell as well as inter-cell interferences. As the number of BS antennas is increased, the value of BER drops since it is inversely proportional to SINR. As discussed earlier, the SINR grows logarithmically with the number of BS antennas. Hence, the BER decays logarithmically. This means that the intra-cell interferences are reduced as the number of BS antennas grows therefore leading to less causes of bit errors. Figure 19 shows how PiC increases the ratio of BER achieved in its presence over BER achieved in its absence, as the number of BS antenna array grows. For instance, when the number of BS antennas is 80, the BER in the presence of PiC is about 1600% of the average BER

in the absence of PiC. Whereas, when the number of BS antennas is increased to 140, the average BER in the presence of pilot contamination is about 2125% of the average BER in the absence of PiC. This means that increasing the number of antennas significantly increases the effect of PiC on the BER hence reducing the performance of the network in terms of BER.

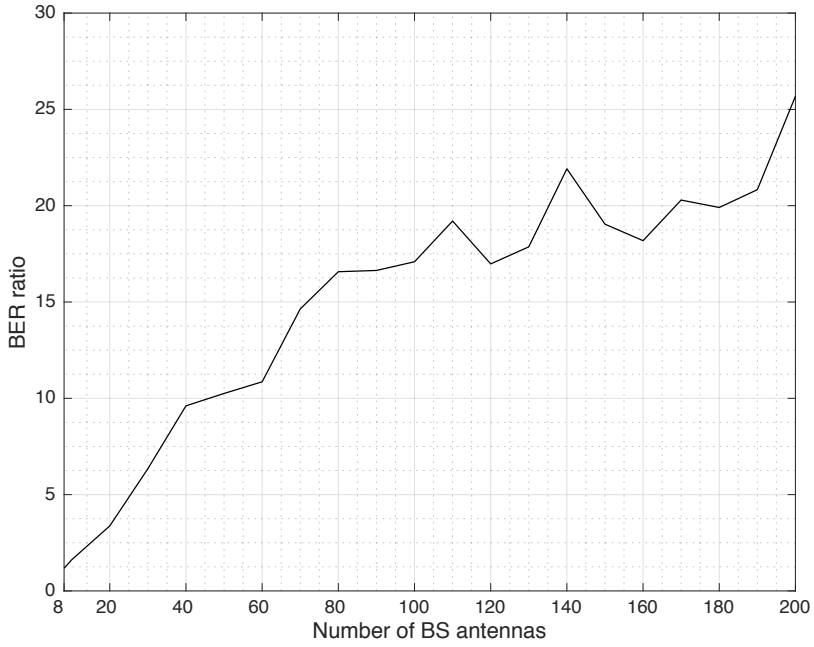

Figure 19. Effect of PiC on the bit error rate.

Observations made in the analysis of the average sum capacity and the average BER interestingly indicate that as the BS antenna array grows, the effect of PiC on the latter increases while the effect on the former decreases. Hence, increasing the number of BS antennas, in the presence of PiC, will improve the overall performance of the network however, the impact of PiC on the sum capacity will be reduced at the cost of increasing its impact on the BER.

4.2. Conclusion and future work

The objective of this thesis was to study the effect of pilot contamination on the performance of massive MIMO systems and to highlight some of the proposed precoding techniques that mitigate pilot contamination. Among the various precoding techniques, it has been established that DPC is the optimal transmission scheme. However, due to its complexity, because of its non-linear nature, it is not a practical scheme. Hence, the theoretical performance of DPC sets the benchmark for the proposed linear schemes.

The effect of pilot contamination has been studied through MATLAB simulations. The analysis has been carried out in the worst case scenario where the UE in the desired cell are on the cell edges. Results showed that as the cluster size increases, inter-cell interferences that cause pilot contamination are significantly reduced since the co-channel cells are further away hence the interferences are weakened. In the scenario where the cluster size is one, meaning the co-channel cells are bordering the desired cell, the probability of the edge users being in outage is increased by a considerable amount. Likewise, the average sum capacity and the BER are significantly lowered. Furthermore, as the BS antenna array grows, the effect of pilot contamination on the average sum capacity gradually reduces while with the probability of outage and BER it increases. Conclusively, novel precoding techniques that mitigate pilot contamination are highly important in massive MIMO networks where the number of BS antennas is very large.

For future work, it is recommended to compute the output SINR at the receiver for better analysis. This is the SINR of the signal after equalization. In this work, only the input SINR was computed (SINR before equalization). Additionally, it is recommended to compute the BER through Monte Carlo simulations that count the number of bits received in error. For simplicity, the BER in this work is computed theoretically.

5. LIST OF REFERENCES

Ashikhmin, Alexei & Thomas Marzetta (2012). Pilot Contamination Precoding in Multi-cell Large Scale Antenna Systems. In: *2012 IEEE International Symposium on Information Theory Proceedings (ISIT)* [online], 1137 – 1141. IEEE [cited 19 July 2016].

Ashikhmin, Alexei, Thomas L. Marzetta & Liangbin Li (2014). *Interference Reduction in Multi-Cell Massive MIMO Systems I: Large-Scale Fading Precoding and Decoding* [online]. arXiv preprint arXiv:1411.4182. [cited 19 July 2016].

Bhatia, V., B. Mulgrew & D.D. Falconer (2007). Non-parametric maximum-likelihood channel estimator and detector for OFDM in presence of interference. *IET Communications* [online] 1:4 [cited 23 October 2016], 647 – 654. ISSN 1751-8636.

Björnson, Emil, Mats Bengtsson, & Björn Ottersten (2014). Optimal Multiuser Transmit Beamforming: A Difficult Problem with a Simple Solution Structure [Lecture Notes]. *IEEE Signal Processing Magazine* [online] 31:4 [cited 23 October 2016], 142 – 148. ISSN 1053-5888.

Chellappa, Rama & Sergios Theodoridis (2013). *Academic Press Library in Signal Processing* [online]. Oxford, United Kingdom: Academic Press [cited 27 June 2016]. ISBN: 9780123972248.

Chockalingam, A. & B. Sundar Rajan (2014). *Large MIMO Systems* [online]. New York, United States of America: Cambridge University Press [cited 27 June 2016]. ISBN: 9781107720589.

Cisco (2016). *Cisco Visual Networking Index: Global Mobile Data Traffic Forecast Update, 2015–2020* [online].

Costa, Nelson & Simon Haykin (2010). *Multiple-Input Multiple-Output Channel Models: Theory and Practice* [online]. Hoboken, New Jersey: John Wiley & Sons, Inc. [cited 04 July 2016]. ISBN: 9780470399835.

Elijah, Olakunle, Chee Yen Leow, Abdul Rahman Tharek, Solomon Nunoo & Solomon Zakwoi Iliya (2015a). A Comprehensive Survey of Pilot Contamination in Massive MIMO - 5G System. *IEEE Communications Surveys & Tutorials* [online] 18:2 [cited 04 Aug 2016], 905 – 923. ISSN: 1553-877X.

Elijah, Olakunle, Chee Yen Leow, Abdul Rahman Tharek, Solomon Nunoo & Solomon Zakwoi Iliya (2015b). Mitigating pilot contamination in massive MIMO system — 5G: An overview. In: *2015 10th Asian Control Conference (ASCC)* [online], 1 – 6. IEEE [cited 22 July 2016].

Jose, Jubin, Alexei Ashikhmin, Thomas L. Marzetta & Sriram Vishwanath (2011). Pilot Contamination and Precoding in Multi-Cell TDD Systems. *IEEE Transactions on Wireless Communications* [online] 10:8 [cited 27 July 2016], 2640 – 2651. ISSN 1536-1276.

Kosbar, Kurt L., William H. Tranter, Theodore S. Rappaport & K. Sam Shanmugan (2003). *Principles of Communication Systems Simulation with Wireless Applications* [online]. New Jersey, United States of America: Prentice Hall [cited 15 August 2016]. ISBN: 9780134947907.

Larsson, Erik G., Ove Edfors, Fredrick Tufvesson & Thomas L. Marzetta (2014). Massive MIMO for Next Generation Wireless Systems. *IEEE Communications Magazine* [online] 52:2 [cited 25 June 2016], 186–195. ISSN: 0163–6804.

Liu, Binyue, Yong Cheng & Xiaojun Yuan (2015). Pilot contamination elimination precoding in multi-cell massive MIMO systems. In: *2015 IEEE 26th Annual International Symposium on Personal, Indoor, and Mobile Radio Communications (PIMRC)* [online], 320 – 325. IEEE [cited 27 July 2016].

Marzetta, Thomas L. (2015). Massive MIMO: An Introduction. *Bell Labs Journal* [online] 20 [cited 25 June 2016], 11–22. ISSN: 1089–7089.

Monserrat, Jose F., Mischa Dohler & Afif Osseiran (2016). *5G Mobile and Wireless Communications Technology* [online]. Cambridge, United Kingdom: Cambridge University Press [cited 23 Jun. 2016]. ISBN: 9781316653166.

Neumann, David, Michael Joham & Wolfgang Utschick (2015). CDI Precoding for Massive MIMO. In: *Proceedings of SCC 2015; 10th International ITG Conference on Systems, Communications and Coding* [online], 1 – 6. IEEE [cited 05 Aug 2016].

Panzner, Berthold, Wolfgang Zirwas, Stefan Dierks, Mads Lauridsen, Preben Mogensen, Kari Pajukoski & Deshan Miao (2014). Deployment and Implementation Strategies for Massive MIMO in 5G. In: *2014 IEEE Globecom Workshops (GC Wkshps)* [online], 346 – 351. IEEE [cited 24 July 2016].

Rodriguez, Jonathan (2015). *Fundamentals of 5G Mobile Networks* [online]. West Sussex, United Kingdom: John Wiley & Sons [cited 23 June 2016]. ISBN: 9781118867525.

Santos, Raul A., Arthur Edwards-Block & Victor R. Licea (2013). *Broadband Wireless Access Networks for 4G* [online]. United States of America: IGI Global [cited 25 June 2016]. ISBN: 9781466648883.

Taha, Abd-Elhamid M., Najah Abu Ali & Hossam S. Hassanein (2012). *LTE, LTE-Advanced and WiMAX: Towards IMT-Advanced Networks* [online]. West Sussex, United Kingdom: John Wiley & Sons [cited 27 June 2016]. ISBN: 9781119970453.

Xu, Peng, Dongming Wang & Jinkuan Wang (2015). Joint Use of H-inf Criterion in Channel Estimation and Precoding to Mitigate Pilot Contamination in Massive

MIMO Systems. In: *2015 IEEE Global Communications Conference (GLOBECOM)* [online], 1 – 6. IEEE [cited 09 Aug 2016].

Zuo, Jun, Jun Zhang, Chau Yuen, Wei Jian & Wu Luo (2015). Multi-cell Multi-user Massive MIMO Transmission with Downlink Training and Pilot Contamination Precoding. *IEEE Transactions on Vehicular Technology* [online] PP:99 [cited 24 July 2016], 1. ISSN 0018-9545.